Letter

The Discovery of BMS-641988, a Novel Androgen Receptor Antagonist for the Treatment of Prostate Cancer

Aaron Balog, Richard Rampulla, Gregory Martin, Stanley Krystek, Ricardo Attar, Janet Dell-John, John D DiMarco, David Fairfax, Jack Z Gougoutas, Christian Holst, Andrew Nation, Cheryl Rizzo, Lana Rossiter, Liang Schweizer, Weifang Shan, Steven H. Spergel, Thomas Spires, Georgia Cornelius, Marco Gottardis, George L Trainor, Gregory D. Vite, and Mark Salvati

ACS Med. Chem. Lett., **Just Accepted Manuscript** • DOI: 10.1021/acsmedchemlett.5b00173 • Publication Date (Web): 19 Jun 2015

The Discovery of BMS-641988, a Novel Androgen Receptor Antagonist for the Treatment of Prostate Cancer

Aaron Balog[§]*, Richard Rampulla[§], Gregory S. Martin[#], Stanley R. Krystek[§], Ricardo Attar[§], Janet Dell-John[§], John D. DiMarco[§], David Fairfax[#], Jack Gougoutas[§], Christian L. Holst[#], Andrew Nation[§], Cheryl Rizzo[§], Lana M. Rossiter[#], Liang Schweizer[§], Weifang Shan[§], Steven Spergel[§], Thomas Spires[§], Georgia Cornelius[§], Marco Gottardis[§], George Trainor[§], Gregory D. Vite[§] and Mark E. Salvati[§]

[§]*Bristol Myers-Squibb Research and Development, P. O. Box 4000, Princeton, NJ 08543*

[#]*Albany Molecular Research Inc., 21 Corporate Circle, Albany, NY 12203*

RECEIVED DATE (will be automatically inserted after manuscript is accepted).

Abstract: BMS-641988 (**23**) is a novel, non-steroidal androgen receptor antagonist designed for the treatment of prostate cancer. The compound has high binding affinity for the AR and acts as a functional antagonist *in vitro*. BMS-641988 is efficacious in multiple human prostate cancer xenograft models, including CWR22-BMSLD1 where it displays superior efficacy relative to bicalutamide. Based on its promising preclinical profile, BMS-641988 was selected for clinical development.

Carcinoma of the prostate (CaP) is the most common malignancy among men in the US and the 2nd most common cause of cancer-related death worldwide after lung cancer.[1] The androgen receptor (AR) is a member of the nuclear hormone superfamily of ligand-induced transcription factors and is a key signaling pathway leading to the emergence of CaP. Androgen ablation, by surgical or chemical castration in combination with an antiandrogen such as hydroxyflutamide (**1**) or bicalutamide (**2**), has been the standard of care for advanced CaP for many years.[2] This therapy is initially effective in 80-90% of patients, however >50% of the patients will ultimately develop castration resistant prostate cancer (CRPC) after ~18 months.[3] The treatment of CRPC is challenging due to the sustained AR signaling, which is the result of AR overexpression/activation and the presence of activating AR mutations.[4] Furthermore, it has been reported that CRPC tumors express the necessary cytochrome P450 enzymes for intratumoral androgen production, thus by-passing the effects of chemical castration which targets only gonadal androgen production.[5] These findings suggest that CRPC remains AR dependent and effective therapies must target AR signaling directly with improved next-generation AR antagonists.

MDV3100 (enzalutamide, **3**) is a potent AR antagonist that was recently approved by the US Food and Drug Administration for the treatment of metastatic CRPC patients that have progressed post treatment with docetaxel.[6] Although enzalutamide has shown promise in treating these patients, nearly all pateints go on to develop resistance to enzalutamide via AR mutations.[4] Thus, there is a need for novel antiandrogens with distinct interactions in the AR ligand binding domain that could be dosed together or sequentially in the clinic to combat the potential pathways leading to CRPC progression. Our laboratory has been focused on the rational strucutral-based design of structurally novel, non-steroidal small molecule AR antagonists for the potential treatment of CRPC.

Figure 1. Known androgen receptor antagonists.

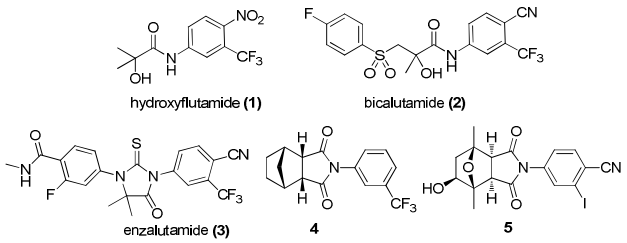

Previously, we have reported a series of [2.2.1] carbobicyclic[7] and oxabicyclic[8] succinimide based AR antagonists (**4** and **5**, Figure 1). These compounds demonstrated potent binding affinity (Ki) and functional antagonist activity (IC_{50}) against the wild-type AR as found in the MDA-MB-453 cell-line (Table 1). These compounds compared favorably in terms of potency to the clinically used antiandrogens hydroxyflutamide (**1**) and bicalutamide (**2**). We designed a series of oxabicyclic-based AR antagonists, such as **5**, that demonstrated a superior pharmacokinetic (PK) profile compared to the carbocycles such as **4**. Based on our understanding of the need for sustained AR supression in an effective AR antagonist, we expected that robust PK would be essential for an efficacious AR antagonist.[8] Accordingly, compound **5** was shown to be efficacious in the CWR22-BMSLD1 human prostate cancer xenograft model, where bicalutamide shows only limited efficacy.[8] We looked to incorporate PK properties critical for an effective AR antagonist, such as log T1/2, with a broader activity profile than is seen with 1st generation agents such as bicalutamide. Accordingly, we screened out agents against the human CaP model CWR22, which has been shown to be refractory to both bicalutamide and hydroxyflutamide. Based on this result, we wanted to expand the scope of this series by using a structure-based approach to identify even more potent AR antagonists.

Utilizing available X-ray co-crystal structures of the AR generated at BMS, we developed a molecular model of the WT AR LBD (Figure 2) to aid in the indentification of new AR antagonists.[9,10] In this model, interactions of N-705 with both the C-5 hydroxyl and the bridging oxygen of compound **5** are evident. Additional interactions between R752 and Q711 and the aryl nitrile functionality of compound **5** are also present. We postulated that endo-substitution at C-5 or C-6 of the bicycle would result in a direct interaction with helix-12 (H-12), possibly creating a more classical AR antagonist conformation, similar to that predicted for bicalutamide. The key

hydrogen bonding interaction with N-705 would be maintained by the bridging oxygen as seen with bicalutamide (**2**) which is shown in orange. Thus, we set out to investigate the effect of various substitutions on the endo-face of [2.2.1]-oxabicyclic core of compound **5**.

Figure 2. Compound **5** docked into a model of the wild-type AR ligand binding domain.

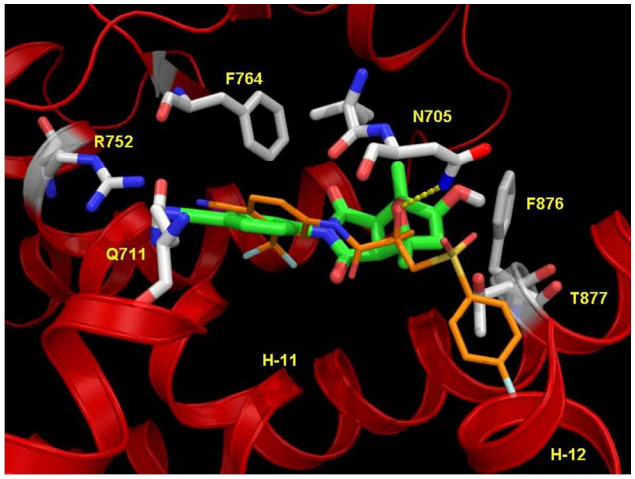

Our efforts started with the synthesis of compounds **11-13** by the synthetic route shown in Scheme 1. Maleimide **8** was prepared from the aniline **6** and maleic anhydride (**7**) under standard conditions.[11] Diels-Alder cycloaddition between **8** and the MEM ester of 2,5-dimethyl-3-furoic acid occurred at 120 °C to give only the desired exo-isomer **9** after precipitation. Catalytic hydrogenation led to formation of the endo-ester by selective reduction from the beta-face of the olefin. Normal-phase chiral HPLC separation of the racemic endo-ester gave the desired enantiomer **10** in 45% yield and >99% ee. The optical isomer depicted by compound **10** was determined to be optimal for potent AR antagonist activity and the absolute and relative stereochemistry was eventually confirmed by X-ray crystallographic analysis of compound **23**.[12] Treatment of **10** with 3N HCl gave the key intermediate acid **11** in good yield. Compounds **12** and **13** were prepared by standard ester and amide formation conditions.

The acid **11** was found to have poor potency in our cellular *in vitro* assays (Table 1), but the ester **12** and amide **13** had promising binding and functional antagonist activity in the MDA-MB-453 cell-line. Unfortunately, neither the amide nor the ester had potency that was superior to the exo-hydroxy analog **5**, so we investigated additional functionalities on the oxabicycle in an effort to find highly potent AR antagonists. The endo-amine **14** could be prepared from the acid **11** by sequential Curtius rearrangement[13] and subsequent TFA-promoted cleavage of the resulting Teoc-carbamate in 77% yield. Compound **14** had only modest affinity to the AR, but offered a good handle with which to further functionalize the oxa-bicyclic core.

Scheme 1. Synthetic route to endo-substituted bicycles

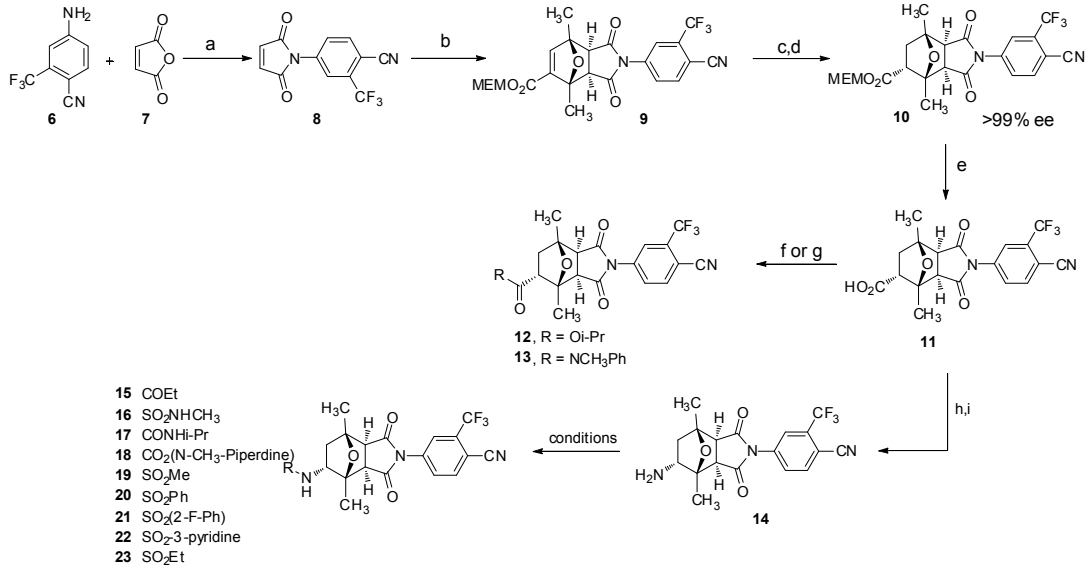

a) HOAc, 110 °C, 88%; b) MEM 2,5-dimethyl-3-furoate, 120 °C, 33%, exo-isomer only; c) H_2, Pd/C, EtOAc, 1 atm, 50%; d) Chiral HPLC separation, 45%, >99% ee; e) 3 N HCl, THF, 22 °C, 98%; f) $(COCl)_2$, DCM then i-PrOH, TEA, 97%; g) EDC, HOBt, DIEA, N-methylaniline, DMF, 88%; h) 2-trimethylsilylethanol, DPPA, TEA, 4Å MS, 1,4-dioxane, 75 °C, 78%; i) TFA, CH_2Cl_2, 22 °C, 99%;

A series of amides, sulfamides, carbamates, ureas and sulfonamides was prepared from the amine **14** in library format. Standard coupling techniques were utilized to prepare analogs **15-23** (see Supporting Information); the corresponding *in vitro* biological data is shown in Table 1. In general, these analogs were potent binders to, and functional antagonists of, the wild-type AR present in the MDA-MB-453 cell line. The amide **15** and the carbamate **18** had excellent potency *in vitro*, while the sulfamide **16** and

urea **17** were weakly active. The sulfonamides **19-23** had the best overall *in vitro* profile, with robust affinity and potent antagonist activity, superior to that for bicalutamide (**2**).

We next wanted to investigate the pharmacodynamic effects of these novel AR antagonists *in vivo*. Compounds **13-23** were progressed into the immature rat prostate weight (IRPW) PK/PD model, where the compound effect on AR dependent growth of the prostate and seminal vesicles was measured (Table 2).[14] In this model, compounds were dosed orally once a day at 1 or 10 mg/kg for 4 days with plasma concentrations of drug measured 2 hours post-dose on day 4. Agents that effectively block the proliferative effect of the AR in these tissues would result in a decrease in the total weight of organs relative to a control group. As expected, the amide **13** had poor pharmacodynamic effect in this model, most likely due to modest functional antagonist potency. The amide **15** and the urea **17** gave only modest PD effects even with very high exposure after 1 and 10 mg/kg doses. This result correlated with the very high serum protein binding measured for these two compounds (>99% in mouse serum). The sulfonamide **16** and the carbamate **18** also had only modest PD effects, but this was most likely due to poor exposure relative to compound **2**. The sulfonamide series stood out in the IRPW model by having excellent PD with modest exposure, suggesting superior *in vivo* potency compared to the ureas, amides, carbamates and sulfamides. Compounds **19-23** all demonstrated robust PD at a 10 mg/kg dose with exposures significantly less than observed for bicalutamide. Of these promising analogs, the ethyl sulfonamide **23** was chosen for further studies due to robust potency *in vivo* and a promising PK profile in rats.

Table 1. In vitro biological activity

#	MDA-MB-453 Ki (nM)[a]	MDA-MB-453 IC_{50} (nM)[b]
2	64	173
5	8	10
11	1600	>5000
12	23	22
13	50	34
14	31	60
15	3.0	23
16	50	34
17	31	60
18	7.0	6
19	12	20
20	10	1.0
21	1.0	10
22	2.0	7.0
23	1.7	16

[a]Binding (Ki) determined through direct displacement with [^{3}H]-DHT in the MDA-MB-453 cell-line

[b]Functional antagonist activity (IC_{50}) in the MDA-MB-453 cell-line determined through a transiently transfected reporter system utilizing the secreted alkaline phosphatase reporter gene driven by the AR-dependent PSA promoter.

Compound **23** was further profiled to determine in vitro safety and ADME properties (Table 3). Inhibition of human cytochrome P450 (CYP) isoforms is very weak (>40 μM) and there is very low potential for CYP induction based on the human PXR transactivation assay. Plasma protein-binding of **23** was measured by equilibrium dialysis and very low levels of plasma protein binding were observed in all species (>10% free). Compound **23** demonstrated excellent metabolic stability in hepatocyte incubations and the predicted clearance in all species is low, especially for human. Finally, the PK properties of compound **23** were assessed in mouse, rat and dog following both oral and IV doses. Consistent with the predicted hepatic clearance, compound **23** demonstrated moderate to long half-lives and very low clearance across species.

Table 2. Immature rat prostate weight assay results

#	IRPW 1 mg/kg SV/FB[a]	IRPW 10 mg/kg SV/FB[a]	Exposure 1 mg/kg (μM)[b]	Exposure 10 mg/kg (μM)[b]
2	69 ± 24	41 ± 4	2.3 ± 0.4	9.5 ± 1.4
13	88 ± 19	43 ± 8.0	1.8 ± 0.68	12.0 ± 0.82
14	89 ± 22	89 ± 8.1	0.08 ± 0.02	0.48 ± 0.32
15	87 ± 39	34 ± 6.0	24 ± 1.7	190 ± 73
16	89 ± 5.9	36 ± 4.2	0.01 ± 0.001	0.23 ± 0.08
17	115 ± 3.9	56 ± 8.9	8.3 ± 0.4	60 ± 6.1
18	105 ± 24	87 ± 16	0.012 ± 0.004	0.076 ± 0.017
19	64 ± 13	26 ± 4.2	0.29 ± 0.07	4.0 ± 1.2
20	63 ± 14	31 ± 5.2	0.23 ± 0.03	2.4 ± 0.52
21	56 ± 6.5	24 ± 1.8	0.16 ± 0.02	1.9 ± 0.06
22	44 ± 8.6	23 ± 11	0.05 ± 0.01	0.52 ± 0.09
23	58 ± 13	26 ± 3.0	0.79 ± 0.17	4.0 ± 0.42

[a]SV/FB is the percentage of weight of the seminal vesicles over the full body weight of the rat (n=3) where testosterone treated control = 100% and sham = 10%.

[b]Plasma exposure measured 2 hours post-dose on day 4.

Figure 3. In vivo efficacy of compound **23** in the CWR22-BMSLD1 prostate cancer xenograft model.

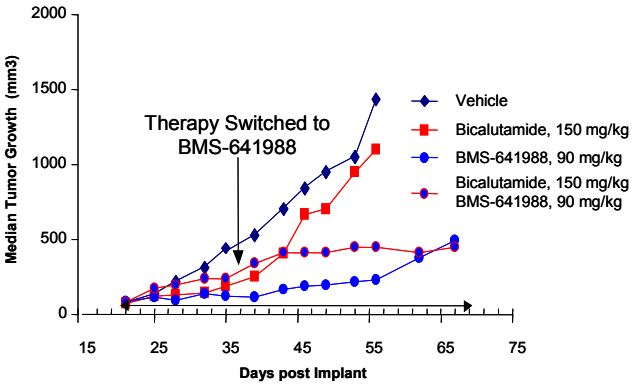

Compound **23** was then tested in the human prostate cancer xenograft model CWR22-BMSLD1 (Figure 3).[15] Treatment with bicalutamide (**2**) (150 mg/kg, po, qd x 35 days) resulted in good tumor growth inhibition for the initial 10 days, followed by regrowth of the tumor at a rate that was similar to control. When compound **23** was dosed (90 mg/kg, po, qd x 45 days) excellent tumor growth inhibition was observed over the entire dosing period, demonstrating superior efficacy to bicalutamide (**2**). Additionally, we investigated the possibility of treating bicalutamide

resistant tumors in this model by allowing the bicalutamide-treated tumors to triple in size followed by a switch to treatment with compound **23**. As shown in Figure 3, tumor growth continued for ~10 days after switching to compound **23**, followed by nearly complete tumor growth inhibition for the remainder of dosing period. We were encouraged by this result as it gave strong evidence that compound **23** has the potential to treat forms of prostate cancer resistant to bicalutamide (**2**).

Figure 4. Compound **23** docked into a model of the WT AR ligand binding domain.

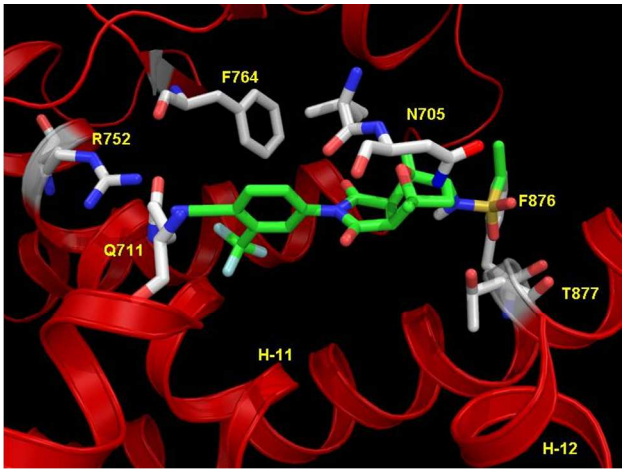

Docking compound **23** into the wild-type AR ligand binding domain (Figure 4)[10] revealed the H-bond from N-705 to the bridging oxygen is likely intact as observed for compound **5**. To accommodate the endo-sulfonamide at C-5, F876 must reorient resulting in a positional shift of Helix-11. This significant shift of Helix-11 results in a change in the overall architecture of the LBD, potentially giving compound **23** the promising antagonist profile presented here.

Further profiling of compound **23** demonstrated an acceptable preclinical safety profile both *in vitro* and *in vivo*. This compound was selected for clinical development and advanced into phase I clinical trials.[15,16]

In summary, we have utilized structure-based design to identify a new series of amino [2.2.1]-oxabicyclosuccinimide AR antagonists. Lead molecules demonstrated potent antagonist activity in cellular binding and transactivation assays *in vitro* and had robust PK/PD profiles in the IRPW model. Compound **23** was shown to be superior to bicalutamide in the CWR22-BMSLD1 human CaP tumor xenograft model, and has the potential to address acquired bicalutamide resistance based on the results from these studies.

Table 3. Summary of androgen receptor biological data and ADME properties for compound **23**

Assay	Results
WT AR binding (Ki)	1.7 ± 0.56 nM
MDA 453 (IC_{50})	16 ± 3 nM
LNCaP (IC_{50})	153 ± 77 nM
human CYP 1A2, 2B6, 2C8, 2C9, 2D6, 3A4) IC_{50}	> 40 μM
PXR-TA EC_{50}	> 50 μM
hERG inhibition @ 30 μM	0 %
Protein binding (% free): mouse, rat, dog, human	14.8, 10.6, 16.5, 10.4
Rate of metabolism in hepatocytes: mouse, rat, dog, monkey, human (pmol/min/10^6 cells)	0, 26, 3.0, 1.0, 2.0
Predicted clearance: mouse, rat, dog, monkey, human (mL/min/kg)	0, 16, 1.8, 0.6, 0.8
IV / PO PK: $T_{1/2}$(h) CL (mL/min/kg), $AUC_{0-\infty}$ (μM*h), %F	
Mouse (5 / 10 mg/kg):	2.4, 4.5, 39.1/74.1, 94.7
Rat (5 / 10 mg/kg):	3.7, 6.5, 31.7/40.5, 63.9
Dog (1 / 2 mg/kg):	21.8, 0.35, 102.1/160.2,79

[a] IC_{50} values are an average of three experiments.

ACKNOWLEDGMENT The authors thank Linda Fleming and the Department of Discovery Synthesis at Bristol-Myers Squibb for preparation of key intermediates. We also acknowledge the Departments of Lead Discovery & Optimization and Discovery Analytical Sciences for ADME and compound characterization support.

Supporting Information Available: Synthetic procedures and characterization data for compounds **9-23** and biological methods. This material is available free of charge via the Internet at http://pubs.acs.org.

References

(1) Ghafoor, A.; Jemal, A.; Thomas, H.; Murray, T. and Thun, M. Cancer statistics for African Americans. *Cancer J. Clin.* **2002**, *52*, 322-325.
(2) Crawford, E. D.; DeAntonio, E. P. Current status of combined androgen blockade: optimal therapy for advanced prostate cancer. *J. Clin. Endocrinol. Metab.* **1995**, *80,* 1062.
(3) Dalesio, O. Maximum androgen blockade in advanced prostate cancer: an overview of the randomized trials. *Lancet*, **2000,** *355,* 1491-1498.
(4) Scher, H.; Sawyers, C. Biology of progressive, castration-resistant prostate cancer: directed therapies targeting the androgen receptor signaling axis. *J. Clin. Oncol.* **2005**, *23*, 8253.
(5) Locke, J. A.; Guns, E. S.; Lubik, A. A.; Adomat, H. A.; Hendy, S. C.; Wood, C. A.; Ettinger, S. L.; Gleave, M. E.; Nelson, C. C. Androgen levels increase by intratumoral de novo steroidogenesis during progression of castration-resistant prostate cancer. *Cancer Res.* **2008**, *68(15),* 6407-6415.
(6) Ning, Y. M.; Pierce, W.; Maher, V. E.; Karuri, S.; Tang, S. H.; Chiu, H.-J.; Palmby, T.; Zirkelback, J. F.; Marathe, D.; Mehrotra, N.; Liu, Q.; Ghosh, D.; Cottrell, C. L.; Leighton, J.; Sridhara, R.; Ibrahim, A.; Justice, R.; Pazdur, R. Enzalutamide for treatment of patients with metastatic castration-resistant prostate cancer who have previously received docetaxel; United States Food and Drug Administration approval summary. *Clin Cancer Res.* **2013**, *19(22)*, 6067 - 6073.
(7) Salvati, M.; Balog, A.; Wei, D.; Pickering, D.; Attar, R.; Geng, J.; Rizzo, C.; Hunt, J.; Weinmann, R. and Martinez, R. Identification of a novel class of androgen receptor antagonists based on the bicyclic-1H-isoindole-1,3(2H)-dione nucleus. *Bioorg. Med. Chem. Lett.* **2005**, *15,* 389.
(8) Salvati, M.; Balog, A.; Shan, W.; Rampulla, R.; Giese, S.; Mitt, T.; Furch, J.; Vite, G.; Attar, R.; J.-K., Maria; Geng, J.; Rizzo, C.; Gottardis, M.; Krystek, S.; Gougoutas, J.; Galella, M.; Obermeier, M.; Fura, A. and Chandrasens, G. Identification and optimization of a novel series of [2.2.1]-oxabicyclo imide-based androgen receptor antagonists. *Bioorg. Med. Chem. Lett.* **2008**, *18,* 1910–1915.
(9) Sack, J. S.; Kish, K.; Wang, C.; Attar, R.; Kiefer, S. E.; Yongmi, W.; Ginger, Y.; Scheffler, J. E.; Salvati, M. E.; Krystek, S. R.; Weinmann, R. and Einspahr, H. R. Crystallographic structures of the ligand-binding domains of

the androgen receptor and its T877A mutant complexed with the natural ligand dihydrotestosterone. *Proc. Natl. Acad. Sci.* **2001**, *98*, 4904.
(10) Molecular modeling was performed using ICM software (Molsoft LLC, San Diego, CA). The docking of the ligands into WT AR LBD was carried out using the ICM docking procedure which is a two step process. Initial docking of ligands were carried out using grid potential representation of the receptor and flexible ligand. Five grid potentials describe the shape, hydrophobicity, electrostatics, and hydrogen bonding potential of the receptor. The conformations from the grid were then optimized with a full atom representation of the receptor and flexible ligand, by an ICM stochastic global optimization algorithm as implemented in version 2.7 of the Molsoft ICM program (Refs. a and b). (a) Molsoft (1998) ICM 2.7 Program Manual (Molsoft, San Diego, CA). (b) M. Totrov and R. Abagyan, *Proteins Suppl. 1* (**1997**), p. 215.
(11) Salvati, M.E.; Balog, A.; Pickering, D.A.; Giese, S.; Fura, A.; Li, W.; Patel, R.; Hanson, R.L.; Mitt, T.; Roberge, J.; Corte, J.R.; Spergel, S.H.; Rampulla, R.A.; Misra, r.; Xiao, H.-Y. Preparation of fused succinimides as modulators of nuclear hormone function. WO 20040077605.
(12) The absolute and relative stereochemistry of compound 23 was confirmed by single-crystal x-ray crystallography. The coordinates have been deposited in the Cambridge Crystallographic Data Center, #779603.
(13) Smith, P. A. S. Curtius reaction. *Org. React.* **1946**, *3*, 337.
(14) Hershberger, L.G.; Shipley, E.G.; Meyer, R.K. Myotrophic activity of 19-nortestosterone and other steroids determined by modified levator ani muscle method. *Proc. Soc. Exp. Biol. Med.* **1953**, *83,* 175.
(15) Attar, R. M. ; Kunkel, M. J.; Balog, A.; Cvijic, M. E.; Dell-John, J.; Rizzo, C. A.; Schweizer, L.; Spires, T. E.; Platero, J. S.; Obermeier, M.; Shan, W.; Salvati, M. E.; Foster, W. R.; Dinchuk, J.; Chen, S.-J.; Vite, G.; Kramer, R.; Gottardis, M. Discovery of BMS-641988, a novel and potent inhibitor of androgen receptor signaling for the treatment of prostate cancer. *Cancer Res.* **2009**, *69*, 6522- 6529.
(16) Rathkopf, D.; Liu, G.; Carducci, M. A.; Eisenberger, M. A.; Anand, A.; Morris, M. J.; Slovin, S. F.; Sasaki, Y.; Takahashi, S.; Ozono, S.; Fung, N. K. E.; Cheng, S.; Gan, J.; Gottardis, M.; Obermeier, M. T.; Reddy, J.; Zhang, S.; Vakkalagadda, B. J.; Alland, L.; Wliding, G.; Scher, H. I. Phase I dose-escalation study of the novel antiandrogen BMS-641988 in patients with castration-resistant prostate cancer. *Clinc. Cancer Res.* **2010**, *17(4),* 880-887.

For Table of Contents use only.

The Discovery of BMS-641988, a Novel Androgen Receptor Antagonist for the Treatment of Prostate Cancer

Aaron Balog[§]*, Richard Rampulla[§], Gregory S. Martin[#], Stanley R. Krystek[§], Ricardo Attar[§], Janet Dell-John[§], John D. DiMarco[§], David Fairfax[#], Jack Gougoutas[§], Christian L. Holst[#], Andrew Nation[§], Cheryl Rizzo[§], Lana M. Rossiter[#], Liang Schweizer[§], Weifang Shan[§], Steven Spergel[§], Thomas Spires[§], Georgia Cornelius[§], Marco Gottardis[§], George Trainor[§], Gregory D. Vite[§] and Mark E. Salvati[§]

Table of Contents Graphic

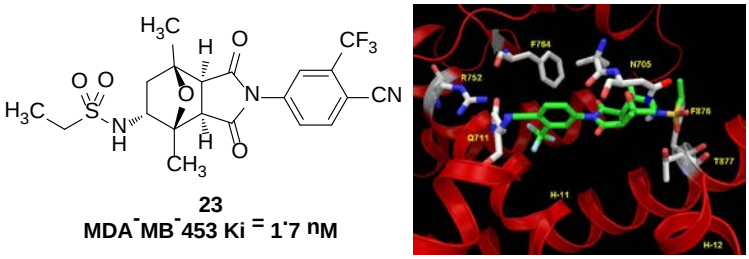

23
MDA-MB-453 Ki = 1.7 nM